JOTCS A
Journal of the Turkish Chemical Society
Section: A
Chemistry
TURKISH CHEMICAL SOCIETY

Pollution Removal Performance of Chemically Functionalized Textile Waste Biochar Anchored Poly(vinylidene fluoride) Adsorbent

Huseyin Gumus[1]*, Bulent Buyukkidan[2]

[1]Bilecik Seyh Edebali University, Osmaneli Vocational School, Bilecik, 11500, Turkey
[2]Kutahya Dumlupinar University, Department of Chemistry, Kutahya, Turkey

Abstract: Preparation of adsorbent materials in powder and polymeric composite form was achieved by controlled carbonization of $ZnCl_2$ pretreated textile waste at low temperatures. Structural and surface properties of carbonized textile waste samples (CTW) and polymeric composites were prepared by the addition of CTW to PVDF-DMF solution at 0, 5, 10, 15, 20, and 30 mass% ratios analyzed by FT-IR, XRD, SEM, and BET analysis. Adsorption performances of powder and composite adsorbents were investigated for MO dye removal from an aqueous solution. Zn-CTW obtained with carbonization of $ZnCl_2$ treated textile waste at 350 ℃ presented 117.5 mg/g MO removal. Those were higher than CTW-350 and CTW-400. The presence of 1545 cm^{-1} band at the IR spectrum of Zn-CTW proved the formation of functional groups that increase dye adsorption performance with honeycomb-like pores on the surface. Zn-CTW reflected its properties onto the PVDF matrix. Improved porosity percentage, BET surface, and dye adsorption of Pz20 were recorded as 105.3, 15.22 m^2/g, and 41 mg/g, respectively, compared with bare PVDF. Disposal of textile waste and preparation of functional activated carbon were achieved in a low-cost and easy way. Zn-CTW loaded PVDF composites are promising materials to use as a dye removal adsorbent from water or filtration membranes.

Keywords: Biochar, carbonization, PVDF composite, waste recycling.

Submitted: November 20, 2021**. Accepted:** April 11, 2022**.**

Cite this: Gumus H, Buyukkidan B. Pollution Removal Performance of Chemically Functionalized Textile Waste Biochar Anchored Poly(vinylidene fluoride) Adsorbent. JOTCSA. 2022;9:777–92.

DOI: https://doi.org/10.18596/jotcsa.1026303.

***Corresponding author. E-mail:** huseyin.gumus@bilecik.edu.tr.

INTRODUCTION

Carbon materials have been preferred as an adsorbent for centuries because of their stability in hard aqueous environments, large surface area, sufficient surface properties for modification as a catalyst, and other applications such as cation exchange capacity and functional groups with low-cost production (1). It is possible to classify the source of carbon materials simply as mineral and biobased according to its obtaining methods. The emerging trend in using carbon sources was through biobased stock materials such as wood and fiber types because of their low cost, high yield, and lower ash content compared with sources of mineral-based (2–4). However, the main preferential reasons for increasing usage of biomaterials for biochar production may be explained by their renewable properties (5,6). Fe_2O_3 modified biochar obtained from the carbonization of maple wood and corn stover, used for H_2S adsorption from biogas, showed 23.9 mg/g H_2S adsorption performance. Thanks to the Fe_2O_3 structure placed into pores, biochar presented good interaction with H_2S (7). Large kinds of biomass are classified basically as woody and nonwoody materials such as bamboo, pecan, peanut nutshell, rice husk, post-harvest residue, and chitosan, which are used to obtain biochar by carbonization techniques called pyrolysis (300-700 °C), hydrothermally (180-300 °C and wetted biomass), torrefaction (<300 °C), gasification (8). Biochar prepared by carbonization of poplar wood and tea by heating at 450 and 750 °C were used for remediation of trichloroethylene (TCE)-contaminated water (9). The best TCE removal was obtained in biochar prepared from poplar wood with 50-100 µm pores, and the highest vinyl chloride removal was obtained from poplar wood carbonized at 750 °C. Modified biochar prepared by castor seed cake for methylene blue (MB) removal (10), activated wakame biochar for MB, rhodamine

blue (RB), malachite green (11), and palm petioles biochar for crystal violet (12) were used as dye adsorbents from aqueous solution with high amounts. Ethylene-co-vinyl alcohol-supported 1.5% rice straw biochar electrospinning membranes showed the highest recovery performance (13). However, the high carbonization temperatures ranging from 450-700 °C, the applied activation methods, and raw biomass usage may be considered as disadvantages of the method. Disposal of carbon-rich waste materials by reducing them to obtain activated carbon can be defined as a further level of environmentalist approach compared with natural biomass usage. Natural biomass can be disposable in the environment, whereas most industrial waste requires extra hard conditions to decompose, and even so, chemical residues can reach soil or water resources. A huge amount of waste material emerges from the textile industry around the world, and disposal problems also threaten the environment. It was reported that 75 percent of textile waste are disposed of in Europe every year due to a lack of efficient recycling and only a small amount of waste textile could be reused as a textile industry due to the necessity of complex separation and purification steps of fibers (14). Textile waste was mainly classified into three groups: specific process waste, secondary waste, and out-of-process waste (15). Carbon-rich textile waste materials consist of synthetic and natural fibers and their residues, such as cotton, polyester yarn, fabric, garments, and fibers, which are included in specific process waste groups, and recycling them has great potential to provide a source of carbon-rich material. Also, that provides environmental protection instead of polluting by stocking or other air polluting methods. The studies dealing with converting textile waste to biogas, ethanol, bio-oil, biofuel, and glycolysis in the presence of single and double oxide catalysts such as Mg-Al were conducted on a lab-scale (16–22). These strategies require a high amount of chemicals such as organic solvents and ionic liquids with the enzymatic reaction, which increases cost and makes applications complicated. Additionally, new waste and chemicals arising from the new system cause a new conflict with the disposal activities of textile waste aimed at environmental protection. A more beneficial strategy may be provided by converting these wastes into valuable bioproducts with low-cost ash and residues. Hanoğlu et al. investigated the effects of fiber type and temperature on the torrefaction of textile fiber at 300-400 °C (23). A significant effect of temperature was reported on the torrefaction process and the energy densification effect of fiber type. Biochar from effluent treatment waste of the textile industry, which has a 91 m^2/g surface area, was prepared for ofloxacin removal from aqueous solutions. Biochar prepared from denim fabric with H_3PO_4 activation presented 19.74 mg/g adsorption capacity as an efficient adsorbent for removing a textile dye from an aqueous solution, and it was separated magnetically from the solution due to magnetic ferrous content (24,25). However, they used a large amount of acid and energy. In another study, the heavy metal content of biochar obtained by carbonization of textile dye sludge at 400-700 °C for disposing of waste sludge was investigated, and the optimum temperature for biochar, which has a minimal toxic effect, was reported as 400 °C with lower heavy metal risk (26). Well-known active carbon preparation methods depend on the heating of natural carbon sources. However, waste materials that are chemical or physical pollutants in case of spreading or staking on the environment may provide a high amount of carbon source. Reusing waste materials has been an important issue for the last three decades, especially due to climate change on a global scale, voiced with agreements (27). Even so, waste recycling is not being applied sufficiently for reasons such as complex structure and specific requirements of waste recycling systems, lack of technology or knowledge, and the easier obtaining of equivalent raw materials. According to our literature survey, we could not come across any studies about the conversion of textile waste that emerged from the Uşak region of Turkey to activated carbon that functional groups decorated at low cost and easy conditions. Also, the preparation and pollution removal studies of chemically functionalized active carbon-polymer composites as a practical adsorbent were first planned and applied in this study.

Conversion of carbon-rich textile waste materials to biochar is applied as an environment protective method for both disposal and new products. The addition of these molecules in a polymer matrix could improve the efficiency of biochar. Thus, easy separation of featured materials such as composite adsorbents or filtration membranes could be achieved. Usable poly(vinylidene fluoride) (PVDF) composites, including carbonized textile waste additives were prepared for dye removal from water. Converting waste materials to biochar with a simple process was investigated with the aim of disposal and environmental protection. The surface, structural properties, and dye removal performance of carbonized textile waste and composites obtained with carbonized samples were investigated. Effects of chemical treatment before carbonization were investigated to obtain well-structured biochar at a lower temperature. Methyl orange removal performance of carbonized samples and composites was investigated at batch experiments, and behaviors of adsorbent in powder form and loaded to PVDF were compared. Although a large amount of research has been conducted to obtain biochar from woody and fiber biomass for different purposes, we aimed to show: (i) the possibility of obtaining fine materials (adsorbent powder and composites) from textile waste with waste specific treatments and conditions, (ii) how important is waste recycling is for the environment, both for disposal and raw material potential. Chemically carbonized textile waste was added to PVDF, and it was used for dye removal in this study. The study includes outcomes focusing on environmental preservation strategies thanks to

biochar preparation steps with moderate conditions. The prepared Zn-CTW added PVDF composites are also promising candidates for filtration and purification systems.

MATERIALS AND METHODS

Materials

Waste textile samples were obtained from UŞAK organized industrial zone, Turkey. C_2H_5OH and $ZnCl_2$ were purchased from Sigma Aldrich and used without any purification. The polymer matrix and solvent were PVDF (Solef 6010, MINGER) and N, N-dimethylformamide, DMF (73.09 g/mol, 0.944 g/mL Sigma Aldrich). During the dye removal experiments, double distilled water, methyl orange (MO, Sigma Aldrich), NaOH, and HCl (Sigma Aldrich) was used for pH adjustments.

Preparation of Carbonized Textile Waste (CTW) Samples and Composites

Waste textile samples were first washed with ethanol and water to remove particles and dye remnants until a clear eluent was obtained. Waste materials were washed and dried at 60°C for 24 h. Five grams of washed sample were wetted by 25 mL $ZnCl_2$ solutions at a mass ratio of activating species: textile waste 0.14-1.4:50 for 1 h. Samples were kept for 24 h at 60 °C in an oven. Dried samples were put into a porcelain cup and carbonized in a muffle furnace (with a heating rate of 15 ℃/min) at temperature ranges of 350-400 ℃ for 1-1.5 h. The air conditions were adjusted with static N_2 inert gas. Control samples were prepared by carbonization of samples at 350 and 400 ℃ without exposure to any chemicals. After cooling to room temperature, carbonized textile waste (CTW) samples were weighed and ground with a manual grinder. Samples were passed through a 150 µm sieve. Obtained samples were called following modification procedures such as 05-Zn-1-350. Where 05 stands for concentration of chemicals (mol/L) used before carbonization, Zn, 1, and 350 for $ZnCl_2$, treatment time, and carbonization temperature, respectively.

Zn-CTW added PVDF composites were prepared as 1,6 g polymer added to 10 mL DMF and stirred for 2 h at 60 °C. Powder 05-Zn-1-350 was added to polymer solution to obtain 0, 5, 10, 15, 20, and 30% Zn-CTW:PVDF mass ratio. The mixture was stirred at 250 rpm at 65 °C for 3 hours to provide homogeneous dispersion. Zn-CTW-PVDF solution was held for a while to avoid air bubbles and cast onto a glass plate (20 cm x 20 cm) with a casting knife with 300 µm at 25 ℃. The mixture was spread onto the glass surface, and it was quickly immersed into the distilled water bath for 24 h. Prepared composites were stored in a storage cup filled with pH 9 distilled water to prevent drying and bacterial contamination until adsorption experiments. Samples were dried and cut into appropriate pieces before structural analysis for optimum results. Composites containing carbonized additives activated by $ZnCl_2$ (Zn-CTW) were called P, Pz5, Pz10, Pz15, Pz20, and Pz30 according to the mass ratio content of Zn-CTW (05-Zn-1-350).

Characterization of carbonized textile waste and composites

Diffraction patterns and organic groups of samples were analyzed by XRD (Rigaku 2000) at 2θ:2°-80° with 2°/min scanning speed and Perkin Elmer FTIR over a range of 4000–400 cm^{-1}. The morphologies of composites were examined by scanning electron microscopy at 10 kV (Carl Zeiss ULTRA Plus). Surface areas of samples were analyzed by the TriStar II 3020 Version 3.02 BET device. After pH adjusting with 0.1 mol/L NaOH/HCl solutions, a 100 ppm methyl orange solution (MO) was prepared and used. The amount of dye content in the solution was determined by a UV-visible spectrometer (Shimadzu, 2550).

Water uptake capacity (WU) of composites was investigated to get knowledge about interactions between virgin PVDF, Zn-CTW added composites, and water. That was useful to estimate their behaviors in the aqueous area during the adsorption. WU calculations were conducted as described: composites in water were mopped slightly with blotting paper and weighted (W_w). Wet samples were dried in a 40 °C vacuum oven for two hours. Dried composites were weighted (W_d) again. Water uptake capacities were calculated by using wet and dry values of composites according to eq. (1).

$$WU(\%) = \frac{W_w - W_d}{W_w} \times 100 \qquad \text{(Eq. 1)}$$

Porosities of composite surfaces (PO%) were calculated by the weight of wet and dry composites. The following equation (2) was used for porosity calculation.

$$PO(\%) = \frac{W_w - W_d}{dA\delta} \times 100 \qquad \text{(Eq. 2)}$$

Where d is the density of water used at 25 ºC, A is the composite area in a wet state (cm^2), and δ is the thickness of composite in wet form (cm) determined by using a thickness gauge (Syntek, ±0.01).

Adsorption Experiments

Adsorption experiments were conducted in a flask by the batch technique. 50 mL aqueous solutions of MO (prepared at 50-150 ppm initial concentrations) were put into a conical glass flask with the adsorbent (0.01-0.1 g adsorbent dosage) and stirred at 150 rpm for 1-3 h. The effects of different temperatures (298-328 K) and pH values (pH 3.00-9.00 of solutions was adjusted by 0.05 mol/L HCl and NaOH solutions) were investigated. After the adsorption equilibrium, adsorbents were filtered, and the filtrate was analyzed with a UV-vis spectrometer at 660 for MO. Adsorption capacity Q_e (mg/g), efficiency E_{AD} (%) of composites, and

CTW adsorbents were calculated by equations 3 and 4 (28).

$$Q_e = \left(\frac{C_0 - C_e}{M} \right) \times V \qquad \text{(Eq. 3)}$$

$$E_{AD}(\%) = \left(\frac{C_0 - C_e}{C_0} \right) \times 100 \qquad \text{(Eq. 4)}$$

Where C_0 and C_e represent initial and equilibrium dye concentrations, M (g) represents the amount of adsorbent, and V (L) is the volume of dye solution. Recycling studies of samples were conducted. Filtrated adsorbents were washed with an acid solution (0.5 mol/L HCl, 25 mL) and rinsed with distilled water until a neutral eluent was obtained. Adsorbents were dried and used for other cycles. This procedure was repeated 5 times. Langmuir and Freundlich isotherm models were applied to evaluate the obtained adsorption data of Zn-CTW by using equations 5 and 6.

$$Q_e = \frac{K_L C_e Q_{max}}{1 + K_L C_e} \qquad \text{(Eq. 5)}$$

$$Q_e = K_f C_e^{\frac{1}{n}} \qquad \text{(Eq. 6)}$$

The maximum adsorption capacities (Q_{max}) and Langmuir constants (K_L) were calculated by using the slope and cutting point of the line of the graph obtained by C_e versus $1/Q_e$. Plotting the graph by $\log_{Q_e}$ versus $\log_{C_e}$Freundlich constant and max adsorption capacity of adsorbents were calculated (29).

RESULT AND DISCUSSION

Characterization of Zn-CTW and Composites

The X-ray diffraction patterns of Zn-CTW and Pz composites are shown in Figure 1. The Zn-CTW showed a single broad peak at around 2θ=8.08, pointing out the semi-crystalline structure of the carbonized sample. Shifting a peak position to a low angle indicates disordered cages and microporosity, whereas an increase in peak strength means an increase in interplanar crystal spacing, which contributes to adsorption (30). Only the small peak at around 2θ=30 may be attributed to the ZnO crystal formed because of using a chemical modification (31). Peaks at around 2θ=18.58, 20.21, and 27.2 indicated characteristic α-phase, and the broad peak, which can be seen clearly at 39.3, corresponds γ-phase of PVDF. The evidence for the β-phase structure of PVDF was determined by broad 2θ=36.46 with a clearly visible 2θ=20.06 peak (32). From the diffraction patterns of composites, the peak strength of the Zn-CTW loaded PVDF matrix has decreased a little bit. The reason for broad peaks was decreasing crystallinity of PVDF with additives. Reduced or lack of crystal structure resulted in a broad peak, which means low strength and nonclear or lower inorganic content (33). From the peak strength of the composites, mixture behaviors of PVDF with Zn-CTW can interfere as Pz-5 has a more homogenous structure than Pz-30. Because of increased Zn-CTW, the characteristic peak of PVDF at around 2θ=18.58 became more visible like it is at virgin PVDF. A combination of Zn-CTW with PVDF at the ratio of Pz5-Pz20 was decided that those have moderate constituents as Zn-CTW-PVDF composites.

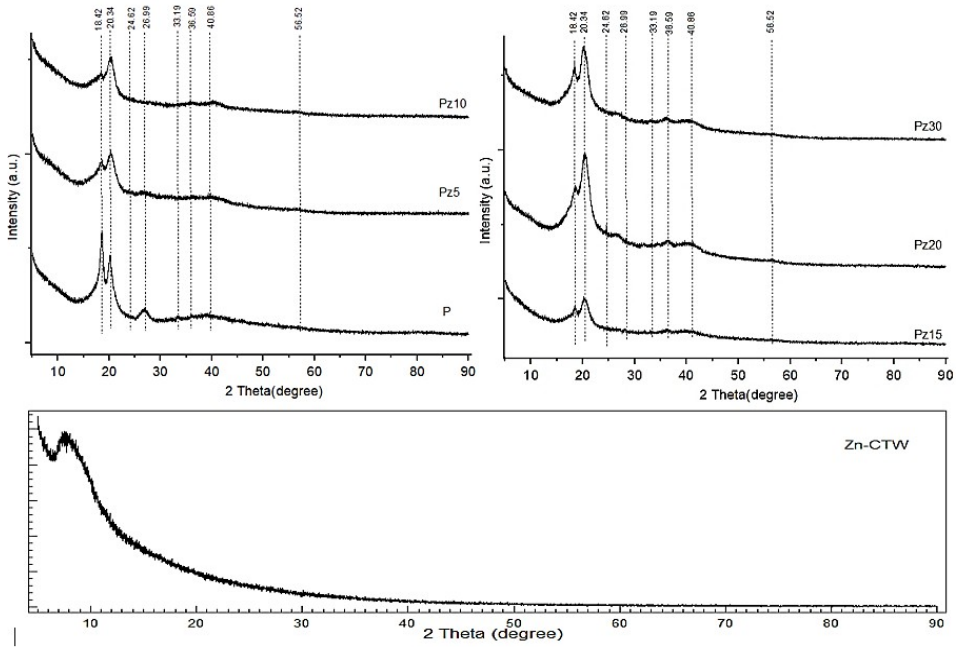

Figure 1: XRD patterns of Zn-CTW and composites.

FT-IR spectra of composites and Zn-CTW are presented in Fig. 2. Typical PVDF bands indicating the CH, CF_2, and CF band stretching vibrations were observed at around 1401, between 875-1180 and 1066 cm^{-1}, respectively. There was no change or disappearance observed at those, except for a shift to a lower wavenumber on a small scale (34). Changes in the IR band positions of PVDF are highly compatible with literature, and those are evidence of phase changes in the structure due to additive interaction. The bands at around 1383, 975, 796, 762, 613, and 531 cm^{-1}, which pointed out α-phases of PVDF, disappeared, or their intensity was reduced prominently with increased addition of Zn-CTW. However, new crystal formations classified as electroactive phases for PVDF appeared interestingly. The band at around 1274 cm^{-1} represents β-phases, with the band at 1234 cm^{-1} (γ-phase of PVDF) emerged and became clear at the FT-IR spectrum of Pz20. (35,36). These findings are important key constituents as they provide knowledge for suitability and loading ratios of Zn-CTW additives to obtain electroactive PVDF products. Successful incorporation of Zn-CTW onto the PVDF chain can be understood by FT-IR bands, which point out the change in PVDF crystal structure. The broad bands of Zn-CTW at around 3059 cm^{-1} may be attributed to OH stretching of physically sorbet water or polysaccharides from cellulosic textile waste.

The presence of carbonyl and alkene groups (C=O and C=C) was understood by stretching bands at 1716 and 1545 cm^{-1}, respectively, due to waste materials' polyester and cellulose structure (23). The intense band at 1094 cm^{-1} corresponds to the C-O-C vibration of organic groups and aromatic stretching and metal oxide bands between 528 and 857 cm^{-1}. (37–39). Morphological analysis of composites and Zn-CTW was done through SEM of the samples' surfaces. Pores of Zn-CTW obtained by carbonization of waste polyester/cotton samples after $ZnCl_2$ treatment can be seen in complex disorganized order in Figure 3a.

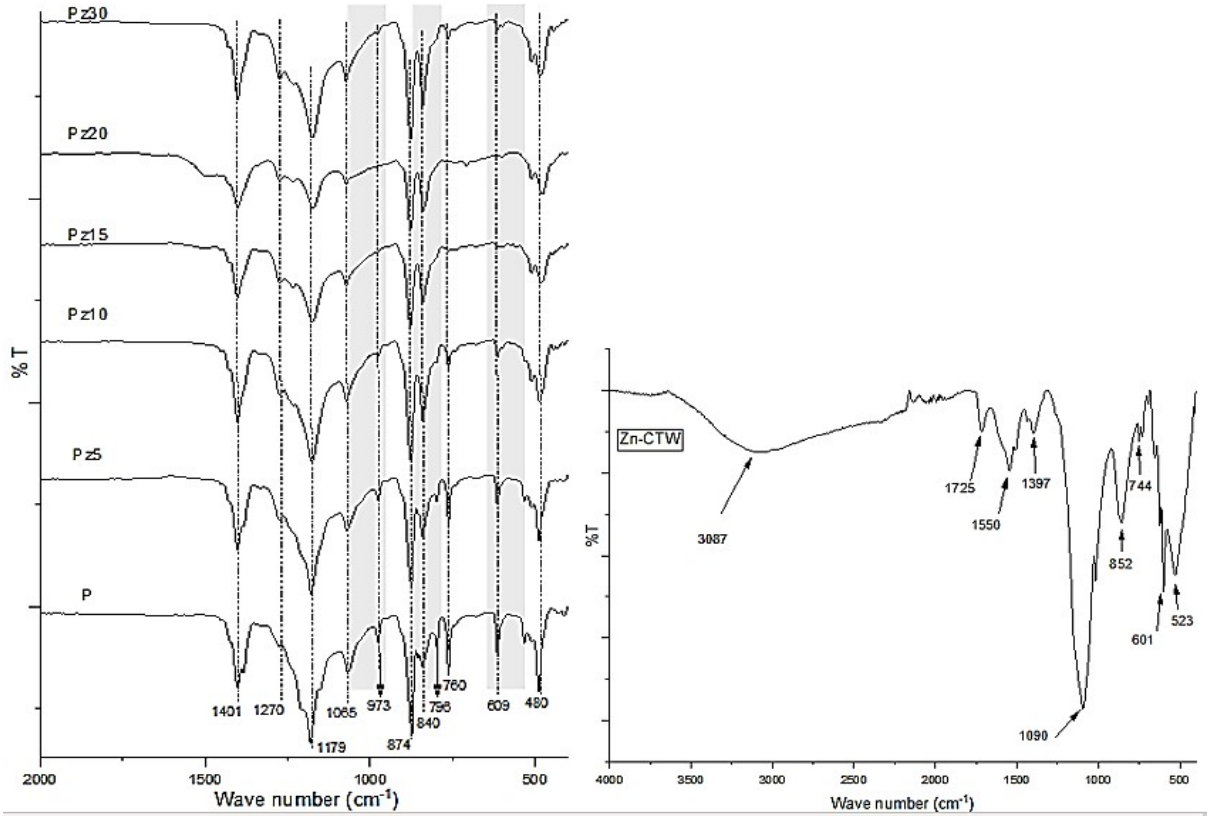

Figure 2: FT-IR spectra of PVDF composites and Zn-CTW.

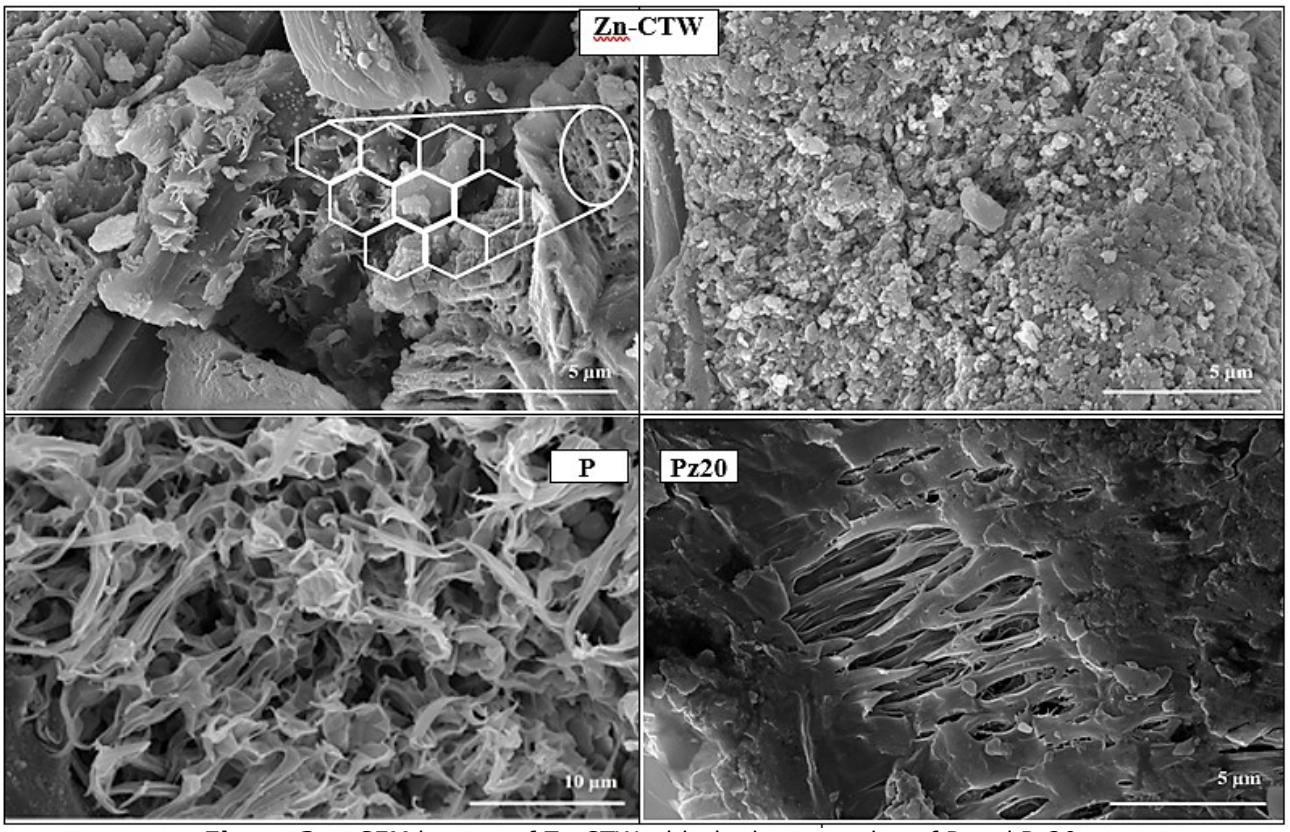

Figure 3a: SEM images of Zn-CTW with the inner section of P and Pz20.

Formations of unburned chemicals and their oxides, such as ZnO, around the channels and surface of the structure could be seen in the images. Also, melted polyesters and cotton remnants that have not burned completely took place inherently in the carbonized samples. Nevertheless, the presence of honeycomb structure was satisfactory evidence of the success of the textile waste carbonization because it provides moderate performance as an adsorbent relatively with its cost-effective and straightforward procedures. Morphological changes in the Zn-CTW loaded PVDF structure were investigated. With increasing additive, the structure became more pressed, and pores turned to narrowed shape inevitably. The amount of Zn-CTW was increased by aiming for the higher performance, but the limit of the performance-additive amount was determined as Pz20. After that, structure heterogeneity increased, and polymer-solid incorporation weakened due to an excess amount of additive. These determinations are compatible and proved with the disappearance of peaks in XRD and FT-IR of Pz30. The inner section of the structure turned into a pressed finger-like compared with the cage-like structure with large space (Fig. 3b).

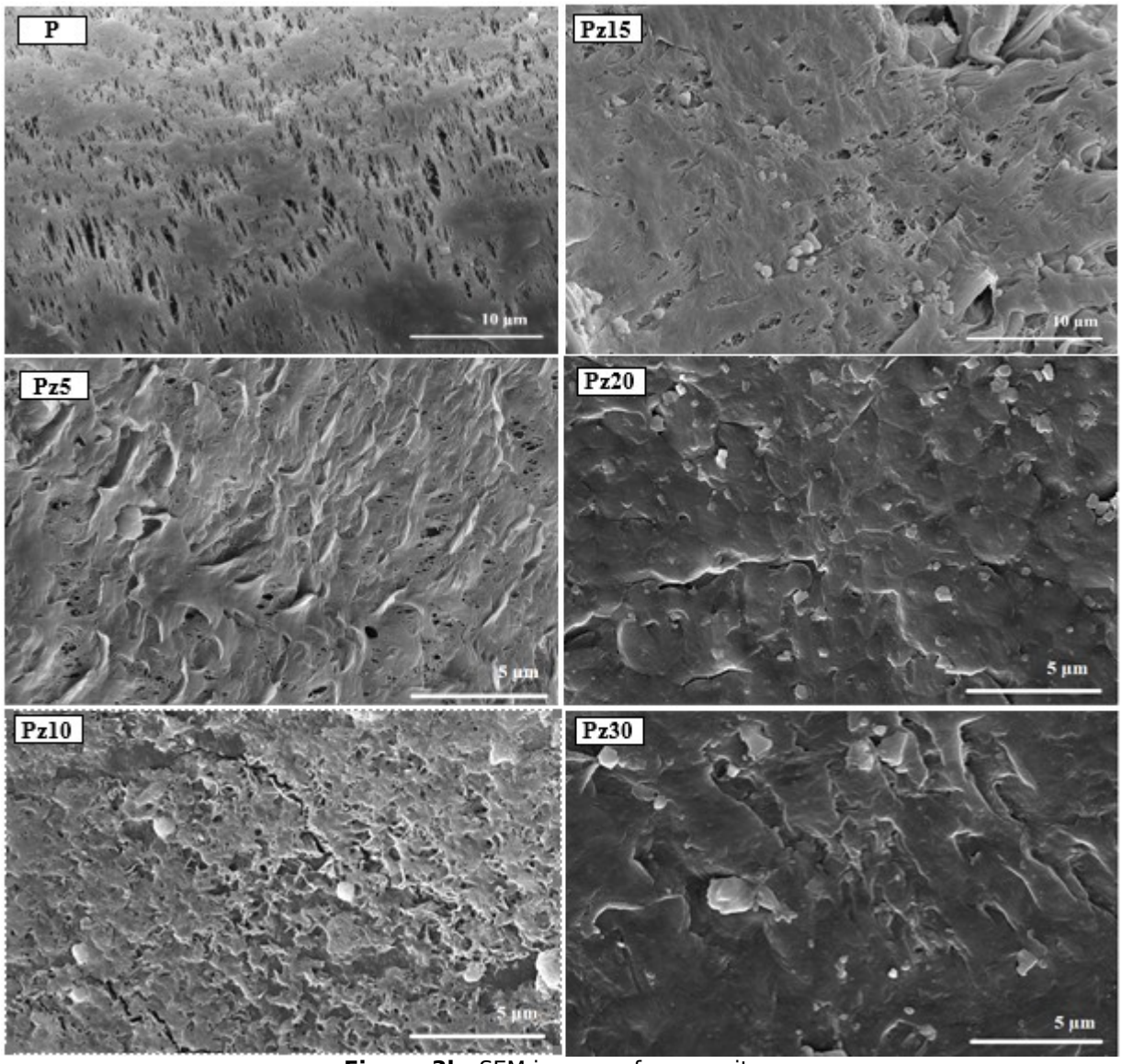

Figure 3b: SEM images of composites.

BET analysis results of samples supported by wettability and porosity data can explain visible shrinkage on the composite structure. Analysis results of Zn-CTW and composites were presented in Table 1. with PO% and WU%.

Table 1: BET area, water uptake (WU%), and porosity percentages of Zn-CTW and composites.

Sample	S_{BET} (m^2/g)	V_{total}(cm^3/g)	Pore width (nm)	WU%	PO%
Zn-CTW	79.5	0.07	3.7	-	-
P	4.11	0.042	6.3	57.2	65.5
Pz5	8.23	0.036	5.8	58.6	65.0
Pz10	8.62	0.017	5.6	56.2	69.2
Pz15	10.42	0.046	5.4	95.7	130.5
Pz20	15.22	0.044	5.7	73.0	105.3
Pz30	7.4	0.036	6.2	45.5	53.3

*S_{BET} :BET surface area
*V_{total} : total pore volume

The effect of the Zn-CTW additive on the surface of composites could be understood from the BET surface of Pz5-Pz30. Remarkable improvement on the surface of PVDF was achieved with Zn-CTW addition from 4.11 to 15.22 m^2/g for P and Pz20, respectively. This was critical for functional polymeric composites, which have tunable properties depending on their application. The satisfactory surface area of Zn-CTW obtained by heating at a low temperature was obtained at 79.5 m^2/g. Compared with the literature, large pores recorded at 3.7 nm resulted in large holes instead

of a high number of small pores, which also provided a higher surface area (40). Total pore volume increased with additive amounts except for Pz5 and Pz10 and reached 0.046 cm^3/g with Pz15. On the other hand, the surface area of composites regularly increased until Pz20 and then decreased until Pz30. The results I: pore volumes changed with the additive amount and structural adjustment, II: the porosity percentage provides information about pore number (PO%) and water uptake (WU%), which are as crucial as pore width and pore volume for composites. It was seen that when the pore volume decreased, it was tolerated by increased PO%. In another sense, Zn-CTW addition pressed pores but increased pore numbers. The changes in WU% are going together with composites' pore volumes, indicating that pore volume is proportional to water penetrating inside the structure. The highest surface area, however, decreasing WU and PO%, was provided by Pz20. The different behavior of surface area and WU-PO% of Pz20 attributes to well-interacted polymer powder that enables reflection of Zn-CTW surface properties even in the polymer matrix. Because of the pressed and blocked structure, the Pz30 composition had the lowest surface area and WU-PO%.

Dye Adsorption Studies Onto Zn-CTW and Composites

Dye adsorption studies were conducted with MO model chemicals on Zn-CTW and composites. The optimal pH, time, adsorbent dosage, and temperature of MO adsorption on the Zn-CTW were determined. The adsorption performance of Zn-CTW was investigated to compare when it was loaded on to PVDF matrix in terms of MO adsorption. To understand the effect of temperature on the adsorption performance, studies were conducted at 308, 318, and 328 K, but any remarkable increase was not observed. So, 298 K was decided as the adsorption temperature for this study.

Effect of solution pH

Adsorption percentages of Zn-CTW at different pH values are presented in Fig. 4. No remarkable changes were observed at pH ranges between 6-9 for MO adsorption. According to reports, one of the predominant reasons for adsorption is the charge of particles in an aqueous solution and surface (41). The functional groups discussed in section 3.1 in this study, predominantly consisting of organic structures, acted as suitable MO adsorbers. The best conditions for attraction of MO and surface were formed at pH values of 7-8. According to the literature, an adsorbent's electrical repulsion and attraction forces can be estimated using its isoelectric points; however, activated carbons and dyes can be amphoteric, and their surface charge varies with acidity (42). The surface became favorable for adsorption when cationic particles were negatively charged at higher pH values from the isoelectric point. MO behaviors in aqueous solution pH 7.44 were determined as favorable, but free electrons of dye with delocalized π-electrons of surface effectively changed the surface charge, and optimum pH of adsorption may shift to different values. The 7.44 pH value was adjusted for aqueous solutions.

Effect of adsorbent dosage

The effect of adsorbent dosage was investigated using a 100 mg/L MO solution and is presented in Fig. 5 in the units of both percentage and mg/g. 43% adsorption performance increased to 71% (142 mg/g) with an increased amount of adsorbent from 10 to 50 mg. That was explained simply by the high number of adsorption sites of Zn-CTW. However, with increased adsorbent amounts, the adsorption percentage reached saturation, and it was recorded at 149, 153, and 158 mg/g for 75, 100, and 150 mg adsorbents, respectively. By considering the Zn-CTW amounts in composites, 50 mg was preferred as a favorable dosage for this study.

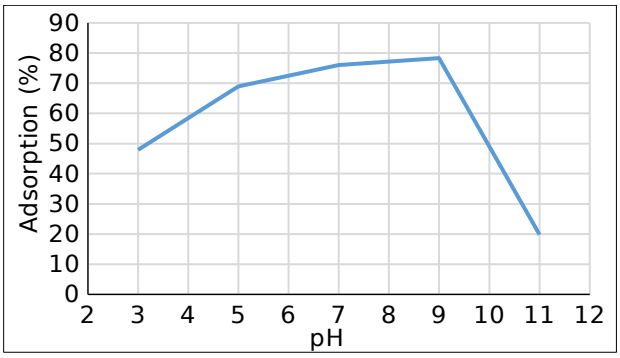

Figure 4: Effect of solution pH on the MO adsorption of 50 mg Zn-CTW with 100 mg/L dye concentration for 1 h contact time at 298 K.

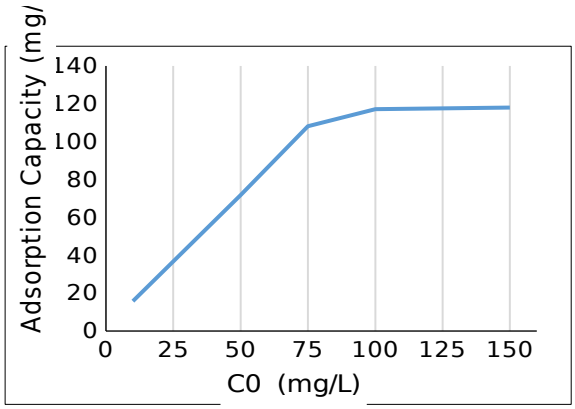

Figure 4: Effect of solution pH on the MO adsorption of 50 mg Zn-CTW with 100 mg/L dye concentration for 1 h contact time at 298 K.

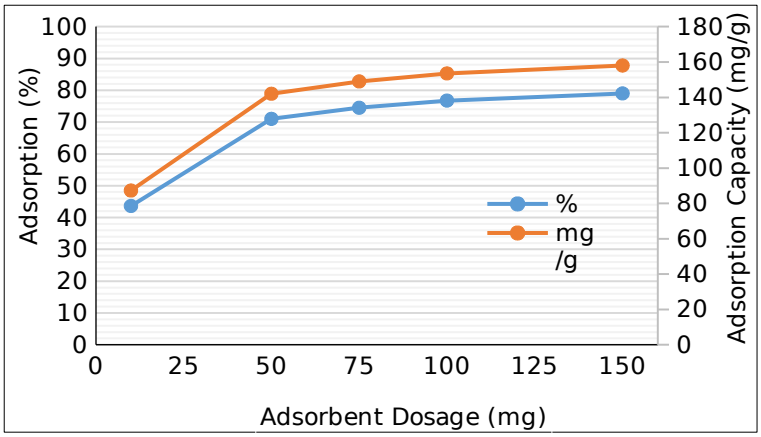

Figure 5: Effect of adsorbent dosage (in terms of removal% and mg/g) on the MO adsorption of Zn-CTW with 100 mg/L dye concentration for 1 h contact time at 298 K..

Effect of contact time and dye concentration

The effects of dye concentration and contact time were given separately in Figures 6a and 6b. From the results, the highest adsorption was obtained when the initial concentration was 100 mg/L with 50 mg of adsorbent. The presence of a large number of adsorption sites resulted in high adsorption. With increased MO, adsorption decreased due to saturation compiled with an explanation of increased adsorbent dosage. The difference between the usual trend of increased adsorption with increased initial concentration may be attributed to the low interaction of vacancies and occupied sites on the surface. Thus, MO particles are adsorbed without affecting the repulsive forces of adsorbed molecules.

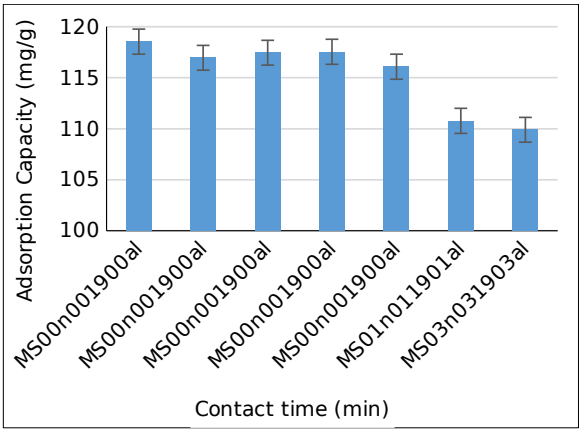

Figure 6: Effect of initial dye concentration for 1 h (a) and contact time (b, dye concentration:100 mg/L) on the MO adsorption of 50 mg Zn-CTW at 298 K.

When the concentration increased, a small increase was recorded after 100 mg/L. Another reason for the low motion of particles that could not adhere to the surface, although the high concentration may be the pH of the studied aqueous. The pH of the studied aqueous may also be a factor in the low motion of particles that could not adhere to the surface. As explained in "effect of pH" (section 3.2.1), MO can be assumed to be charged with neutral or very low anionic and cationic forms at the studied pH. Contact time and adsorption capacity values are presented in Fig 6b, and 120 min was considered the optimum time for adsorption studies for Zn-CTW.

Adsorption performance of Zn-CTW and composites

MO dye adsorption capacities of composites from aqueous solutions were investigated, and the results are presented in Fig. 7. MO adsorption capacity of composites generally increased from Pz5-Pz20. MO adsorption of Pz5 was 59 mg/g while it was 24 mg/g for P. The Zn-CTW additive increased MO adsorption by inducing the formation of new pores and channels and in addition to the adsorption capability of the additive. The importance of regular pores and structure has priority compared with the additive rate in terms of adsorption capacity.

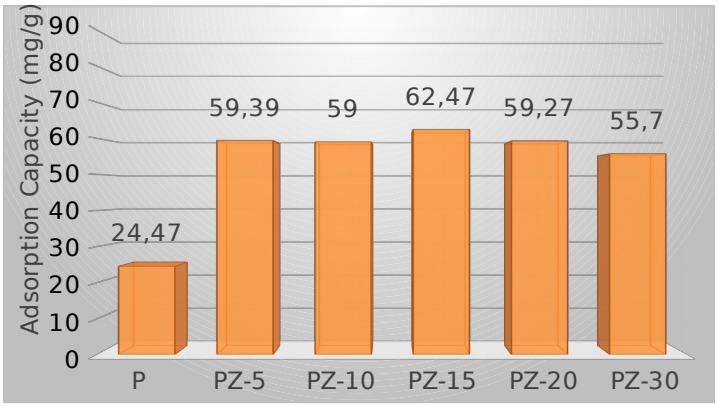

Figure 7: MO dye adsorption performance of composites (adsorbent dosage:50 mg, dye concentration: 100 mg/L, contact time: 2 hours, temperature: 298 K).

As can be seen, the MO adsorption capacity of composites decreased with increased amounts (after PZ-15). It reached the lowest with Pz30 due to its impressed structure. Adsorption decreased as the trapped structure prevented the aqueous solution from entering the composite surface. On the other hand, the MO model dye solution only consisted of basic MO molecules. Therefore, it is estimated that the dye removal performance of composites from industrial wastewater may be different as they contain particles of different sizes in addition to dye.

The bare additive amount loaded onto the PVDF matrix should be considered in addition to the formation of polymer structure induced by the additive. Even if the entire mass of Zn-CTW is loaded into PVDF, there are lots of parameters that affect adsorption performance inside the polymer matrix. It can be inferred that the dye adsorption mechanism onto polymeric composite includes significant differences from traditional solid adsorbents, which was the aim of this study. The composite pore, structure, and interaction with the aqueous solution are highly important for the adsorption performance of the composite. Pz15-Pz20 combinations were decided to be the best Zn-CTW and PVDF compositions for this study.

Adsorption isotherms

Isotherm models that are useful for estimating the interaction between particles and surface were applied to adsorption data. Equilibrium dye concentration and adsorption capacity of only powder form Zn-CTW adsorbent were used for Langmuir and Freundlich isotherm models according to equations 7 and 8 (43). Thus, it is aimed to learn whether the MO adsorption on the powder surface conforms to the adsorption isotherms. The structural differences inherent in the composite surface require investigation of which isotherm the composite adsorption fits the best. This should be discussed in detail in a different study.

$$\frac{C_e}{Q_e} = \frac{1}{K_L Q_{max}} + \frac{C_e}{Q_{max}} \qquad \text{(Eq. 7)}$$

$$\log_{Q_e} = \log_{K_f} + \frac{1}{n} \log_{C_e} \qquad \text{(Eq. 8)}$$

Where C_e (mg/L), the concentration of dye in the eluent after adsorption, Q_{max}: max adsorption capacity of sorbent, K_f, n and K_L are the constants of isotherm of Freundlich and Langmuir models respectively at equilibrium. From the R^2 values presented in Table 2.

Table 2: Isotherm parameters of Zn-CTW for MO adsorption.

	Langmuir Isotherm				Freundlich Isotherm		
	Q_{max} (mg/g)	K_L (L/mg)	R_L	R^2	K_f ($mg^{1-n}/g\ L^n$)	n	R^2
Zn-CTW	135.13	0.0992	0.1969	0.9829	0.33	0,6486	0.8717

It was understood that the adsorption mechanism matched the Langmuir model determined by monolayer adsorption on a homogeneous surface. According to the Langmuir model, Q_{max}, the max adsorption capacity of the adsorbent was found to be 135.13 mg/g. That could be seen as reasonable in terms of mechanism and experimental results. Although it is a low-cost process, Zn-CTW performed over moderate adsorption capacity than other adsorbents obtained from biomass and textile waste. The value of the dimensionless constant separation factor called R_L is a constant to explain the feasibility of the Langmuir isotherm and was also calculated by Eq. 9 (44).

$$R_L = \frac{1}{1 + b C_0} \quad \text{(Eq. 9)}$$

In a sense, R_L is an indicator of the shape of the isotherm. If R_L=1, that means the isotherm is linear; if R_L>1, it is unfavorable, and when R_L=0 or 0<R_L<1, that means the isotherm is irreversible and favorable, respectively. R_L value of 0.1969 for Zn-CTW is evidence of the feasibility of adsorption as favorable.

When considering the amount of Zn-CTW loaded onto PVDF and composite performance, it can be understood that Zn-CTW provided high adsorption capacity to the polymer matrix. The adsorbent dosage was adjusted as 0.05 g for Zn-CTW and composites, although composite contains a small amount of Zn-CTW (approximately 15% of total mass). The well interaction of the polymer and additive was responsible for the improvement effect of Zn-CTW loading onto PVDF. That gives rise to proper pores, channels, and surfaces rather than simply attaching additives to the polymer. Obtained composite is a promising agent as a pollution removal agent for filtration material for ultrafiltration or other applications.

Advantages of Chemical Activation on Carbonization and Adsorption

Biomass usage to prepare adsorbent materials is a preferred method to get low-cost raw materials. Converting carbon-rich materials to activated carbon has the potential of a couple of benefits: disposal of waste and preparation of activated carbon. Converting the textile waste to valuable products economically requires investigation of the yielded procedures according to their structure. Textile wastes consisting of polyester and cotton mixture were handled and carbonized. It was concluded that carbonized samples with chemical activation showed high adsorption of MO. These can be explained by high surface area, crystallinity, porous structure, and functional surface groups observed in the analysis spectra. Chemical activation induced the formation of C=O and OH, NH groups, which are highly effective in adsorption on the surface of the carbonized sample. Zn^{2+} and a small amount of ZnO acted as catalysts, and functional groups increased. The higher catalytic activity of Zn^{2+} than ZnO was reported for n-butane to n-butene transformation even at lower temperatures (45). The transformation mechanism advanced on the Zn^{2+}....-O^{2-} acid-base pair may be proposed for polyester-cellulose textile waste. That continued with the adsorption of substrates on the Lewis acid-base pair, the formation of zinc-substrate intermediates, electron transfer, and the formation of yield (46).

The presence of Zn accelerated the carbonization, and more organic structures decomposed at 350 °C. Compared with Zn activated and nonactivated samples, the ash remnant of Zn activated samples is less than others with higher adsorption performance (Table 3).

Additionally, the absence of functional groups was understood at CTW-350 and CTW-400 surfaces from the IR bands attributed to C=C and C-O-C vibrations at 1545 and 1094 cm^{-1}, as shown in Figure 8. Concerned with all findings such as functional groups, porous honeycomb structure, and adsorption capacity, chemical activation is necessary to decrease temperature and obtain activated carbon with a modified structure.

Table 3: Remnant (after carbonization) and MO adsorption performances of CTW.

Sample	Mass%	MO%
Zn-CTW	67.1	74.8
CTW-350	28	27.6
CTW-400	13.8	52.5

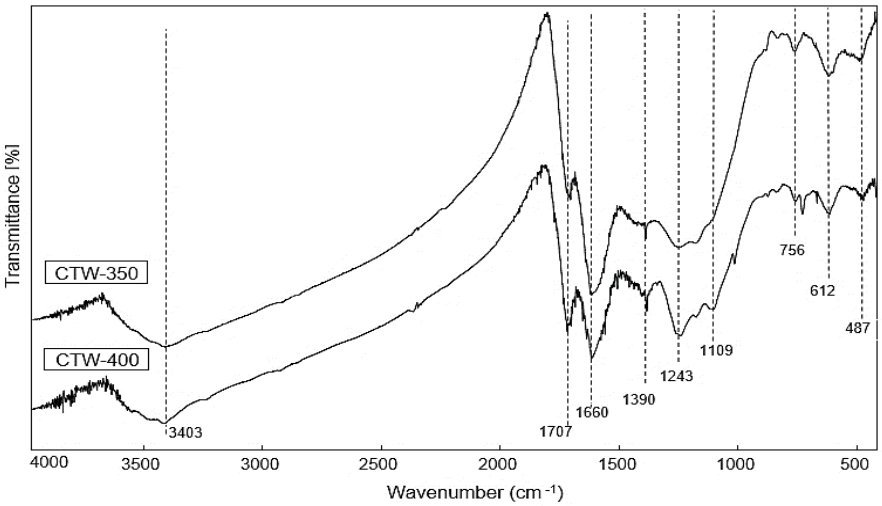

Figure 8: FT-IR spectra of activated carbons obtained at 350 (CTW-350) and 400 °C (CTW-400) without chemical pretreatment.

Regeneration

The reusability of adsorbents was tested after washing as described in section 2.4. After 4 cycles of MO adsorption and desorption, there was no observed decrease in the adsorption capacity of samples (Figure 9). Even a small amount of increase was observed for regenerated Zn-CTW after acid treatment. Washing with an acidic solution may break off some species locked in the pores with adsorbed dye molecules and result in a well transporting structure.

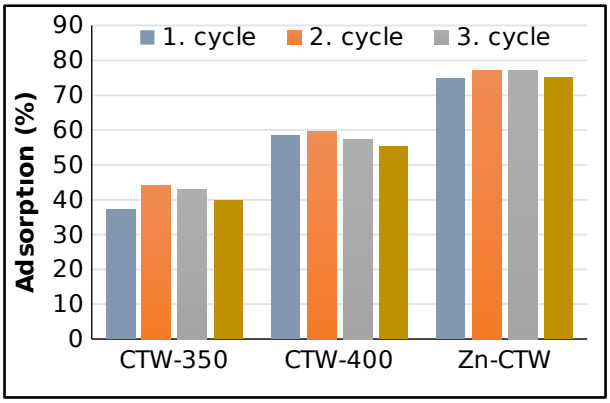

Figure 9: Reusing performance of 350 (CTW-350),400 °C (CTW-400), and Zn-CTW.

CONCLUSION

Carbonization of $ZnCl_2$ pretreated textile waste samples was conducted. Their structure, surface, and dye adsorption properties were investigated. The obtained sample was loaded into the PVDF matrix to understand the usability of its adsorption properties inside composites for different applications. Chemical activated samples showed better porosity, water uptake, and noticeable structural adjustment for high adsorption of MO. 05-Zn-1-350 (Zn-CTW) has 117 mg/g MO dye adsorption performance. Composites obtained by adding 0, 5, 10, 15, 20, 25, and 30% Zn-CTW were investigated for an additive effect on the structure and dye adsorption performance. Interaction of additive with PVDF chain was determined by decreasing XRD peak strength that showed α-phase PVDF at around 2°=18.58, 20.21, and 27.2 with IR bands of 1383, 975, 796, 762, 613, and 531 cm^{-1}. The optimum additive amount was decided as 15-20% due to increased structural strain and adsorption capacity until that ratio. Polymeric composites consist of two or more kinds of different combinations of materials to improve the properties of polymeric structure and gain easy usage as powder. Zn-CTW added PVDF provided increased adsorption performance compared with raw PVDF. That made it preferable for different applications, such as filtration or pollution removal from water. Biochar prepared by simple chemical activation could show triple effects. Upon disposal of textile waste, obtaining moderately featured activated carbon acted as an additive material for composite preparation.

CONFLICT OF INTEREST

The authors have no conflicts of interest to declare relevant to this article's content, and all authors agree that the study should be published.

ACKNOWLEDGMENTS

We would like to thank the Chemistry Department of the University of Kütahya Dumlupinar for their support in providing the laboratory equipment. This work was financially supported by the Department of Scientific Research Project (Dept. of Kütahya DPU BAP) at the University of Kütahya Dumlupinar (No. 2020-08).

REFERENCES

1. Vieira O, Ribeiro RS, Pedrosa M, Lado Ribeiro AR, Silva AMT. Nitrogen-doped reduced graphene oxide – PVDF nanocomposite membrane for persulfate activation and degradation of water organic micropollutants. Chem Eng J [Internet]. Elsevier; 2020;402(March):126117. Available from: <DOI>.

2. Pala M, Kantarli IC, Buyukisik HB, Yanik J. Hydrothermal carbonization and torrefaction of grape pomace: A comparative evaluation. Bioresour Technol. 2014;161:255–62. <DOI>.

3. Arteaga-Pérez LE, Segura C, Bustamante-García V, Cápiro OG, Jiménez R. Torrefaction of wood and bark from Eucalyptus globulus and Eucalyptus nitens: Focus on volatile evolution vs feasible temperatures. Energy. 2015;93:1731–41. <DOI>.

4. Tag AT, Duman G, Ucar S, Yanik J. Effects of feedstock type and pyrolysis temperature on potential applications of biochar. J Anal Appl Pyrolysis. 2016;120:200–6. <DOI>.

5. Ambaye TG, Vaccari M, van Hullebusch ED, Amrane A, Rtimi S. Mechanisms and adsorption capacities of biochar for the removal of organic and inorganic pollutants from industrial wastewater. Int J Environ Sci Technol [Internet]. Springer Berlin Heidelberg; 2020; Available from: <DOI>.

6. De Oliveira GF, De Andrade RC, Trindade MAG, Andrade HMC, De Carvalho CT. Thermogravimetric and spectroscopic study (Tg-DTA/FT-IR) of activated carbon from the renewable biomass source babassu. Quim Nova. 2017;40(3):284–92. <DOI>.

7. Choudhury A, Lansing S. Adsorption of hydrogen sulfide in biogas using a novel iron-impregnated biochar scrubbing system. J Environ Chem Eng [Internet]. Elsevier Ltd; 2020;9(1):104837. Available from: <DOI>.

8. Yaashikaa PR, Kumar PS, Varjani S, Saravanan A. A critical review on the biochar production techniques, characterization, stability and applications for circular bioeconomy. Biotechnol Reports [Internet]. Elsevier B.V.; 2020;28:e00570. Available from: <DOI>.

9. Della L, Ducousso M, Batisse N, Dubois M, Verney V, Xavier V, et al. Poplar wood and tea biochars for trichloroethylene remediation in pure water and contaminated groundwater. Environ Challenges [Internet]. Elsevier B.V.; 2020;1(August):100003. Available from: <DOI>.

10. Silva RVS, Gonçalves AD, Vinhal JO, Cassella RJ, Santos RC, Sasso MAD, et al. Bioproducts from the pyrolysis of castor seed cake: basic dye adsorption capacity of biochar and antifungal activity of the aqueous phase. J Environ Chem Eng. 2020;9(August 2020):104825. <DOI>.

11. Yao X, Ji L, Guo J, Ge S, Lu W, Chen Y, et al. An abundant porous biochar material derived from wakame (Undaria pinnatifida) with high adsorption performance for three organic dyes. Bioresour Technol [Internet]. Elsevier; 2020;318(September):124082. Available from: <DOI>.

12. Chahinez HO, Abdelkader O, Leila Y, Tran HN. One-stage preparation of palm petiole-derived biochar: Characterization and application for adsorption of crystal violet dye in water. Environ Technol Innov [Internet]. Elsevier B.V.; 2020;19:100872. Available from: <DOI>.

13. Ali NA, Hussein EA. Characterization of functional electrospun polymeric nanofiber membranes. Int J Environ Sci Technol [Internet]. Springer Berlin Heidelberg; 2019;16(12):8411–22. Available from: <DOI>.

14. Haslinger S, Hummel M, Anghelescu-Hakala A, Määttänen M, Sixta H. Upcycling of cotton polyester blended textile waste to new man-made cellulose fibers. Waste Manag [Internet]. The Author(s); 2019;97:88–96. Available from: <DOI>.

15. Anonim. Sektörel Atık Kılavuzları. 2016;146.

16. Nautiyal P, Subramanian KA, Dastidar MG. Experimental investigation on adsorption properties of biochar derived from algae biomass residue of biodiesel production. Environ Process. 2017;4:S179–93. <DOI>.

17. Jeihanipour A, Aslanzadeh S, Rajendran K, Balasubramanian G, Taherzadeh MJ. High-rate biogas production from waste textiles using a two-stage process. Renew Energy [Internet]. Elsevier Ltd; 2013;52:128–35. Available from: <DOI>.

18. Jeihanipour A, Karimi K, Niklasson C, Taherzadeh MJ. A novel process for ethanol or biogas production from cellulose in blended-fibers waste textiles. Waste Manag [Internet]. Elsevier Ltd; 2010;30(12):2504–9. Available from: <DOI>.

19. Xu Z, Qi R, Xiong M, Zhang D, Gu H, Chen W. Conversion of cotton textile waste to clean solid fuel via surfactant-assisted hydrothermal carbonization: Mechanisms and combustion behaviors. Bioresour Technol. 2021;321(November 2020). <DOI>.

20. Kwon D, Yi S, Jung S, Kwon EE. Valorization of synthetic textile waste using CO2 as a raw

material in the catalytic pyrolysis process. Environ Pollut [Internet]. Elsevier Ltd; 2021;268:115916. Available from: <DOI>.

21. Subramanian K, Chopra SS, Cakin E, Li X, Lin CSK. Environmental life cycle assessment of textile bio-recycling – valorizing cotton-polyester textile waste to pet fiber and glucose syrup. Resour Conserv Recycl [Internet]. Elsevier; 2020;161(May):104989. Available from: <DOI>.

22. Guo Z, Eriksson M, Motte H de la, Adolfsson E. Circular recycling of polyester textile waste using a sustainable catalyst. J Clean Prod [Internet]. Elsevier Ltd; 2020;283:124579. Available from: <DOI>.

23. Hanoğlu A, Çay A, Yanık J. Production of biochars from textile fibres through torrefaction and their characterisation. Energy. 2019;166:664–73. <DOI>.

24. Singh V, Srivastava VC. Self-engineered iron oxide nanoparticle incorporated on mesoporous biochar derived from textile mill sludge for the removal of an emerging pharmaceutical pollutant. Environ Pollut [Internet]. Elsevier Ltd; 2020;259:113822. Available from: <DOI>.

25. Silva TL, Cazetta AL, Souza PSC, Zhang T, Asefa T, Almeida VC. Mesoporous activated carbon fibers synthesized from denim fabric waste: Efficient adsorbents for removal of textile dye from aqueous solutions. J Clean Prod. 2018;171:482–90. <DOI>.

26. Wang X, Li C, Li Z, Yu G, Wang Y. Effect of pyrolysis temperature on characteristics, chemical speciation and risk evaluation of heavy metals in biochar derived from textile dyeing sludge. Ecotoxicol Environ Saf [Internet]. Elsevier Inc.; 2019;168(August 2018):45–52. Available from: <DOI>.

27. Hein J, Guarin A, Frommé E, Pauw P. Deforestation and the Paris climate agreement: An assessment of REDD + in the national climate action plans. For Policy Econ [Internet]. Elsevier; 2018;90(November 2017):7–11. Available from: <DOI>.

28. Li Z, Hanafy H, Zhang L, Sellaoui L, Schadeck Netto M, Oliveira MLS, et al. Adsorption of congo red and methylene blue dyes on an ashitaba waste and a walnut shell-based activated carbon from aqueous solutions: Experiments, characterization and physical interpretations. Chem Eng J. 2020;388(December 2019). <DOI>.

29. Patra C, Gupta R, Bedadeep D, Narayanasamy S. Surface treated acid-activated carbon for adsorption of anionic azo dyes from single and binary adsorptive systems: A detail insight. Environ Pollut. 2020;266. <DOI>.

30. Li L, Fan C, Zeng B, Tan M. Effect of pyrolysis temperature on lithium storage performance of pyrolitic-PVDF coated hard carbon derived from cellulose. Mater Chem Phys. 2020;242. <DOI>.

31. Arularasu M V., Harb M, Vignesh R, Rajendran T V., Sundaram R. PVDF/ZnO hybrid nanocomposite applied as a resistive humidity sensor. Surfaces and Interfaces. 2020;21(September). <DOI>.

32. Saha P, Debnath T, Das S, Chatterjee S, Sutradhar S. β-Phase improved Mn-Zn-Cu-ferrite-PVDF nanocomposite film: A metamaterial for enhanced microwave absorption. Mater Sci Eng B Solid-State Mater Adv Technol [Internet]. Elsevier; 2019;245(April 2018):17–29. Available from: <DOI>.

33. Abdulsalam J, Mulopo J, Oboirien B, Bada S, Falcon R. Experimental evaluation of activated carbon derived from South Africa discard coal for natural gas storage. Int J Coal Sci Technol [Internet]. Springer Singapore; 2019;6(3):459–77. Available from: <DOI>.

34. Gumus H. Performance investigation of Fe 3 O 4 blended poly (vinylidene fluoride) membrane on filtration and benzyl alcohol oxidation: Evaluation of sufficiency for catalytic reactors. Chinese J Chem Eng. Elsevier B.V.; 2019;27(2):314–21. <DOI>.

35. Medeiros KAR, Rangel EQ, Sant'Anna AR, Louzada DR, Barbosa CRH, D'Almeida JRM. Evaluation of the electromechanical behavior of polyvinylidene fluoride used as a component of risers in the offshore oil industry. Oil Gas Sci Technol. 2018;73(2). <DOI>.

36. Cai X, Lei T, Sun D, Lin L. A critical analysis of the α, β and γ phases in poly(vinylidene fluoride) using FTIR. RSC Adv. Royal Society of Chemistry; 2017;7(25):15382–9. <DOI>.

37. Sartova K, Omurzak E, Kambarova G, Dzhumaev I, Borkoev B, Abdullaeva Z. Activated carbon obtained from the cotton processing wastes. Diam Relat Mater. 2019;91(June 2018):90–7. <DOI>.

38. Yedurkar S, Maurya C, Mahanwar P. Biosynthesis of Zinc Oxide Nanoparticles Using Ixora Coccinea Leaf Extract—A Green Approach. Open J Synth Theory Appl. 2016;5(1):1–14. <DOI>.

39. Ahmad F, Daud WMAW, Ahmad MA, Radzi R. Cocoa (Theobroma cacao) shell-based activated carbon by CO 2 activation in removing of Cationic dye from aqueous solution: Kinetics and equilibrium studies. Chem Eng Res Des. 2012;90(10):1480–90. <DOI>.

40. Choi GG, Jung SH, Oh SJ, Kim JS. Total utilization of waste tire rubber through pyrolysis to obtain oils and CO2 activation of pyrolysis char. Fuel Process Technol. 2014;123:57–64. <DOI>.

41. Chiang CH, Chen J, Lin JH. Preparation of pore-size tunable activated carbon derived from waste coffee grounds for high adsorption capacities of organic dyes. J Environ Chem Eng. 2020;8(4). <DOI>.

42. Xiao W, Garba ZN, Sun S, Lawan I, Wang L, Lin M, et al. Preparation and evaluation of an effective activated carbon from white sugar for the adsorption of rhodamine B dye. J Clean Prod. 2020;253. <DOI>.

43. León O, Muñoz-Bonilla A, Soto D, Pérez D, Rangel M, Colina M, et al. Removal of anionic and cationic dyes with bioadsorbent oxidized chitosans. Carbohydr Polym. 2018;194:375–83. <DOI>.

44. Gabrienko AA, Arzumanov SS, Lashchinskaya ZN, Toktarev A V., Freude D, Haase J, et al. n-Butane transformation on Zn/H-BEA. The effect of different Zn species (Zn2+ and ZnO) on the reaction performance. J Catal [Internet]. Elsevier Inc.; 2020;391:69–79. Available from: <DOI>.

45. Gumus H. Catalytic performance of polyvinylidene fluoride (Pvdf) supported TiO2 additive at microwave conditions. J Turkish Chem Soc Sect A Chem. 2020;7(2):361–74. <DOI>.